

ESTIMATION OF SOURCE PARAMETERS OF 2003 BAM (IRAN) EARTHQUAKE FROM ENVISAT SAR IMAGES USING GENETIC ALGORITHM TECHNIQUE

S. Vajedian^a, M. Saradjian^b, M.A. Sharifi^c,

Center of Excellence in Geomatics Eng. and Disaster Management, Dept. of Surveying and Geomatics Eng., College of Eng., University of Tehran -
s_vajedian@yahoo.com,
sarajian@ut.ac.ir
sharifi@ut.ac.ir

Commission VIII, WG VIII/12

KEY WORDS: Satellite Remote Sensing, Earthquakes, Spatial Modeling, Disaster, SAR Image, Radar, Interferometric SAR (InSAR)

ABSTRACT:

In this paper, we analyze synthetic aperture radar (SAR) interferograms derived from Envisat radar data. Use of interferograms from both ascending and descending satellite passes enables us to indicate regions of surface and near-surface slip which is used to modeling procedure. Also we used azimuth offset (AZO) data as additional data. This is horizontal displacement information for earthquake that is obtained with sub pixel matching of SAR amplitude images. Combining the interferometry with subpixel matching of the SAR amplitude images allows us to obtain the full three-dimensional displacement field for the earthquake. We inverted this field to gain insight into the fault geometry and slip distribution of the rupture. Our results indicate that the best fitting dislocation model is a steeply strike-slip fault with maximum of ~3 m that has a size of 12.3 by 8.3 km and strike 355° from north.

1. INTRODUCTION

Active faulting in Iran is result of the convergence between the Arabian & Eurasian plates, which occurs at about 40 mm yr⁻¹ at longitude 60°E and is mostly accommodated by distributed shortening within the political borders of Iran. InSAR applications provides ideal situation for active tectonic studying & seismic hazard assessment in Iran. With the advent of space borne radar systems, SAR interferometry is becoming a new tool for active tectonics by providing both surface change maps spanning periods of days to years, for measuring co- and inter-seismic deformations, and accurate high resolution topographic maps for measuring crustal strain accumulated over longer periods of time. The 26 December 2003 Mw6.5 Bam earthquake is the world's deadliest earthquake to occur for more than a decade; more than 26500 people died. Bam is located only 50 km east of the north-south striking Gowk fault system that has been quite active. [Jónsson, et al 2004]

Several studies have already been carried out to investigate mechanics and source parameters of the Bam earthquake. Wange et al. (2004) inverted descending and ascending interferograms and concluded that the Bam event was a right-lateral strike-slip earthquake that ruptured a total length of about 24 km from south to north crossing the Bam city. FU et al. (2004) used Aster 3-D images and suggested that the Bam event was probably triggered by right-lateral strike-slip faulting on the northern segment of the Bam fault.

Motagh et al (2006) combined precise leveling and InSAR data to constrain source parameters of the earthquake.

In this study we used interferograms and azimuth offset from ascending and descending tracks of Envisat satellite of the European Space Agency associated with the 2003 Bam earthquake. With these three independent observations of

ground displacement, from different viewing geometry, it is possible to construct a three-dimensional displacement field of the deformation due to earthquake.

These 3D field displacements were inverted to gain insight into the fault geometry and slip distribution of the rupture using elastic dislocation model of Okada. In this regard, a rectangular dislocation surface (i.e., a surface across which there is a discontinuity in the displacement vector) was used as a model of a vertical fault.

A set of 7 fault parameters used in our model are: 1) fault length, 2) coordinates of the fault, 3) upper and lower depth, 4) strike, 5) dip, 6) slip and 7) rake. , the goal is to find the values of parameters which best fit the data. There are two approaches in this regards: forward and inverse problem. Estimation of fault parameters with first method is a trial-and-error approach. We used second method; estimation of parameters in this method is done directly from observed data. Fitting the modeled fringe to observed data in this approach is better than forward approach. We intended to solve inverse problem with InSAR data only, without need to any geologic data. In this regards we found Genetic algorithm (GA) as a powerful tool. GA is a search technique used in computing to find exact or approximate solutions to optimization and search problem. This algorithm can estimate unknown parameters without need to know initial value.

2. OBTAINING DISPLACEMENTS FROM ENVISAT ASAR IMAGERY

2.1 InSAR measurements as geodetic data

Like seismograms, geodetic measurements decompose the displacement vector into components. InSAR records only the

component along the line of sight between the satellite and ground point. The line of sight between point on the ground and the radar satellite in the sky define two angles, the radar incidence (from vertical) and the azimuth of the satellite ground track (from north). For Envisat satellites in Iran, for example, these quantities are approximately 23° and 354° . These quantities determine the unit vector \hat{s} which points from ground to satellite. Then the change in range $\Delta\rho$ or the distance measured along the line of sight between the satellite and ground point is

$$-\rho = u \cdot \hat{s}$$

InSAR can provide a second component of the coseismic displacement vector if the satellite acquires two images in both the ascending (south-to-north) and descending (north-to south) orbital passes.

2.2 Data

The synthetic aperture radar (SAR) data used in this study consists of images collected by the European Space Agency (ESA) Envisat spacecraft on 3 December 2003 and 7 January 2004 (Descending pass, Track 120, Frames: 22 and 23, orbits: 9192 and 9693) and on 16 November 2003 and 29 February 2004 (Ascending pass, Track 385, Frames: 21 and 24, orbits: 8956 and 10459).

Orbit	Date
Ascending	
8956	Nov. 16, 2003
10459	Feb. 29, 2004
9958	Jan. 25, 200
Descending	
6687	Jun. 11, 2003
9192	Dec. 3, 2003
9693	Jan. 7, 2004

Table 1. Envisat-ASAR acquisitions used. All were acquired in Swath 2 with VV polarization.

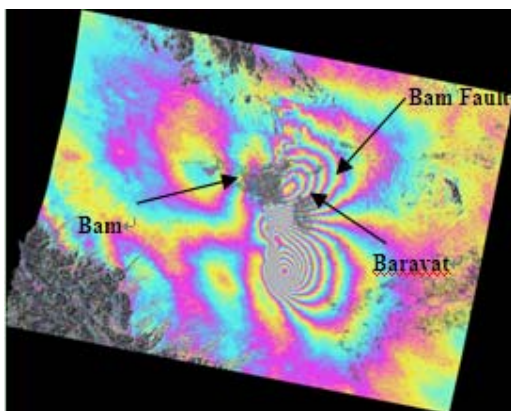


Figure. 1. Coseismic interferogram of the Bam earthquake from a descending orbit. The towns of Bam and Baravat are decorrelated due to damage and vegetation

The European Space Agency (ESA) distributed freely Envisat radar data of the Bam earthquake in early 2004. Acquisitions suitable for interferometric analysis of the Bam earthquake were acquired before and after the earthquake in ascending and descending passes (table1). Unfortunately only the descending acquisitions cover the complete displacement pattern of the event. Figure 1 shows the descending interferogram.

2.3 Data Processing

Data are processed using the public domain SAR processor DORIS developed at Delft Institute for Earth Oriented Space research (DEOS), Delft University of technology.

With the software we could process all the main stages of interferometric processing, from read SLC images and coregistration of them to producing complex interferograms and coherence maps.

In this study we need to retrieve only displacement fringes, so we must subtract the topographic component and other components of the phase in the interferogram. For subtract the topographic component, three-pass interferometry was employed, in this approach 3 radar images of the same area is combined to form two interferograms and then the interferometric phase field due to topography is removed from the observed phase. After removing topographic component, the interferograms were unwrapped using a statistical minimum-cost flow algorithm implemented in a program called SNAPHU, this algorithm unwraps the entire image, which can lead to obvious unwrapping errors, because of this we masked out decorrelated areas.

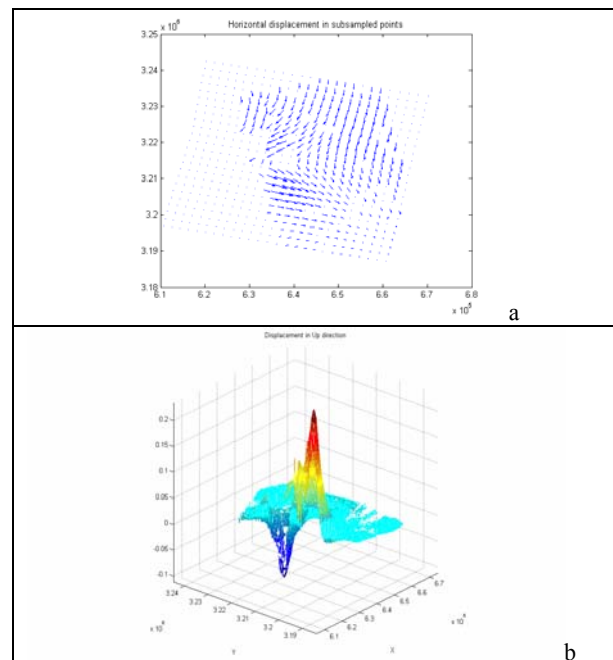


Figure 2 a,b- Vertical and horizontal displacement field calculated from InSAR data, respectively.

We used 2 series interferograms; ascending and descending interferograms which related to descending and ascending satellite passes, respectively. These data enabled us to indicate regions of surface and near-surface slip which is used to modeling procedure. Also we used azimuth offset (AZO) data

as additional data. This is horizontal displacement information for earthquake that is obtained with sub pixel matching of SAR amplitude images. Combining the interferometry with subpixel matching of the SAR amplitude images allows us to obtain the full three-dimensional displacement field for the earthquake, distinguishing vertical from horizontal motions.

The purpose of modeling procedure used here is to determine a set of source parameters explaining both the tectonic observations and the InSAR data.

3. ESTIMATION EARTHQUAKE PARAMETERS BY INVERSION GEODETIC DATA

3.1 The standard elastic half-space model

To explain the observed coseismic deformation, a simple model of a dislocation in an elastic half-space provides a good approximation. Indeed, it has become the conventional model used in most of the case studies. Okada(1985) derives the expression for the coseismic (permanent) displacement u at the earth's surface caused by a fault at depth in closed analytic form. Accordingly, the displacement field $u_i(x_1, x_2, x_3)$ due to a dislocation $\Delta u_j(\xi_1, \xi_2, \xi_3)$ across a surface Σ in an isotropic medium is

$$u_i = \frac{1}{F} \iint_{\Sigma} \Delta u_j \left[\lambda \delta_{jk} \frac{\partial u_i^n}{\partial \xi_n} + \mu \left(\frac{\partial u_i^j}{\partial \xi_k} + \frac{\partial u_i^k}{\partial \xi_j} \right) \right] v_k d\Sigma$$

Where δ_{jk} is the Kroncker delta,, λ and μ are Lamé's coefficient, v_k is the direction cosine of the normal to the surface element $d\Sigma$, and the summation convention applies. The term u_i^j is the i th component of the displacement at (x_1, x_2, x_3) due to the j th direction point force of magnitude F at (ξ_1, ξ_2, ξ_3) . For the complete set of equations see Okada(1985), who also corrects previous derivations.

3.2 Fault parameters

Here we follow Okada's (1985) notation, as in Feigl and Dupre (1999). To describe a single fault element(also called "subfault" or "patch") as a dislocation requires ten parameters. The fault patch has length L and width W . The slip on the fault plane is a vector U with three components, U_1, U_2, U_3 . The position coordinates of the fault patch are E, N and d , taken positive east, north, and down. The azimuth α gives the strike of the fault, in degrees clockwise from north. Finally, an observer facing along strike should see the fault dip at δ degrees to his right.

The Okada parameters differ slightly from the parameters favored by seismologists. In particular, the region of Okada's fault patch does not coincide with the centroid at the geometric center of the fault rectangle (Feigl and Dupre 1999). For a double-couple source, the tensile component vanishes ($U_3=0$) and the slip vector U lies in the fault plane. Seismologists define the rake angle r such that $\tan r = U_2/U_1$ (Aki and Richards, 1980). Inversely, $r = \text{ATAN2}(U_2, U_1)$ where ATAN2 is the intrinsic function for arctangent (U_2/U_1) on the range $[-$

$180, +180]$. A thrust-faulting mechanism, for example, has $U_2 > 0$ and $r > 0$. A normal faulting mechanism, on the other hand, has $U_2 < 0$ and $r > 0$. Similarly, left-lateral slip implies $U_1 > 0$ and $|r| \geq 90^\circ$.

3.3 Underlying assumption

The standard Okada model assumes that Earth's surface is flat, correspondingly to the bounding plane of the elastic half space. The lame coefficient λ and μ specify the elastic medium.

For simplicity, most studies assume that $\lambda = \mu$, so that these parameters drop out of the expression for surface displacement. Such a medium, called a Poisson solid, has a Poisson's ratio of $1/4$, a reasonable approximation to the value of $0.23-0.28$ estimate from P- and S-wave velocities in the upper crust (Perrier and Ruegg, 1973; Dziewonski and Anderson, 1981). The so-called "geometric moment" or "potency" simply equals ULW . To obtain the seismic moment multiply by the shear modulus μ so that $M_0 = \mu ULW$. Typical values (assumed) for μ in the earth's crust range from 30 to 36 GPa, but values as low as 10 GPa (Dal Moro and Zadro, 1999) and as high as 50 GPa (Barrientos and Ward, 1990) have been used. In this paper we used 30 GPa.

3.4 Modeling by inverse method

In our modeling we estimated the geometry of a single fault plane. We used the finite rectangular dislocation embedded in an elastic halfspace. Ten parameters define the dislocation: Location east and north, length, width strike, dip, depth, down-dip extent, and strike-slip and dip-slip across the plane.

The standard Okada model defines the relation between the earthquake source parameters and the geodetic measurements of surface displacement. Here the goal is to find the values of parameters which best fit the data. There are two approaches in this regards: forward modeling and inverse technique. In first approach estimation of fault parameters is done with a trial-and-error approach. In this method best guess for the value of each parameter is used to calculate a synthetic displacement field. Although this modeling can produce accurate models, they require considerable time and expertise (gained mainly by trial and error) to construct and refine. In addition, there is no statistical measure or "proof" that a particular forward model is in fact the best fit to the data. To greatly reduce the effort and time required, and to produce a statistically verifiable best-fit model to the data given the constraints (InSAR data with associated error estimates) an inversion technique is used. Here we used Genetic algorithm (GA) as a powerful tools for inversion. Below we describe the GA algorithm briefly.

3.5 Genetic algorithm

A genetic algorithm (GA) is a search technique used in computing to find exact or approximate solutions to optimization and search problem, which based on the principles of genetics and natural selection. This algorithm starts with definition of initial population that is composed of many individuals; each individual (chromosome) is an array of variable values to be optimized. Number of population is optional. Population represent by a matrix which has $N_{pop} \times N_{var}$ arrays. After this step for survival of the fitness, a large portion of the high cost chromosomes is discarded and chromosomes that are fit enough to survive and possibly enable

to reproduce offspring in the next generation are kept. After determining how many chromosomes can be survived for mating, now is time to select two pairs of chromosomes from mating pool to reproduce new offspring. There are several approaches for this mean. In each generation a number of chromosomes are designated as elite that are destined, and survive unchanged for next generation. In mating process one or more offspring can be created from selected pairs. In the most common form of mating, to parents produce two offspring. A method for this is crossover approach, in this approach for fraction of chromosomes, other than elite, chromosome's genes of parents are combined to create new generation, so that new individual already present in chromosomes range, because of this, crossover step so called exploration. Other method is mutation which in it a GA explores cost surface is mutation approach, which provide genetic diversity and enable the GA to search a border space. Eventually, these process repeat many a time to convergence is achieved.

In this paper we considered ten parameters as genetic unknowns. According to this number each individual (chromosome) of population should have 10 gens. Figure 3-a shows these gens for initial population, in this generation each chromosome was selected randomly. Figure ... shows the initial population. After the algorithm performed for 1000 generations, the algorithm converged. Figure 3-a,b shows the convergence of GA.

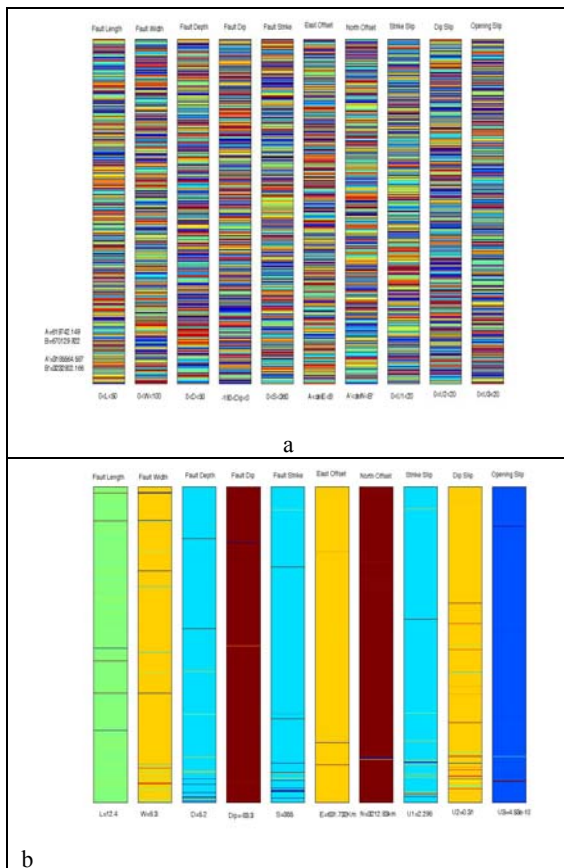


Figure 3-a,b: a: presentation of initial population, the chromosomes were selected randomly for 1000 individuals. b: The population was converged after 1000 generations.

Figure 3-b show the final result of GA for the unknowns, However, the dip-slip parameters(U_3) was found insignificant in the inversion and subsequently fixed to zero. We found that the

best-fitting dislocation model predicts a rectangular fault 12.3 ± 0.1 by 8.3 ± 0.3 km which strikes 355° and dips steeply to the east (dip 83.8 ± 0.8). The optimal fault has a centroid depth of 5.2 ± 0.03 km and slipped up to 2.29 ± 0.01 m right-lateral. The surface projection of the fault is centered at $29.043_N \pm 0.03$ km and $58.360_E \pm 0.01$ km, approximately 4 km east of the previously-mapped Bam fault.

The estimated geodetic moment, $M_0 = \mu AS$, is $6.73 \cdot 10^{18}$ Nm, where A is the fault area, S is slip, and $\mu = 30$ GPa is the shear modulus.

4. CONCLUSION

The Bam earthquake occurred on a near-vertical, north-south striking fault, about 5 km west of the previously mapped Bam fault.

SAR Interferometry data are inverted to gain insight into the fault geometry and slip distribution of the rupture using elastic dislocation model of Okada. The Genetic algorithms have been successfully employed for solving inverse problems in engineering disciplines. In this study, we consider the GAs as an inversion tool for 2003 Bam (Iran) earthquake. The achieved results are quite promising and comparable to previously published results.

Using a reference shear modulus (30 GPa), we find geodetic moment $6.73 \cdot 10^{18}$ Nm, similar to seismic estimates of $6.6 \cdot 10^{18}$ Nm (fast moment tensor solution; USGS (2003)), and $6.8 \cdot 10^{18}$ Nm (teleseismic inversion; YAGI (2003)).

REFERENCES

Okada, Y. (1985). Surface deformation due to shear and tensile faults in a half-space, *Bull. Seism. Soc. Am.* 75, 1135-1154.

Feigle, K.L. and E. Dupre (1999). *Comput. Geosci.* 25, 695-704.

Aki, K. and P.G. Richards (1980). "Quantitative Seismology", Freeman.

Prier, G. and J.C Ruegg (1973). *Ann. Geophys. Res.* 105, 29, 435-502.

Dziewonski, A.M. and D.L. Anderson (1981). *Phys. Earth Planet. Inter.* 25, 297-356.

Jónsson, S, Mai, P.M., Small, D., Meier, E., Salichon, J., Giardini, D. (2004): Using SAR interferometry and teleseismic data to determine source parameters for the 2003 BAM earthquake. Proc. to the Envisat Conferenc European Space Agency

Dal Moro, G. and M. Zadro (1999). *Earth Planet. Sci. Lett.* 170, 119-129.

Barrientos, S.E. and S.N. Ward (1990). *Geophys. J. Int.* 103, 589-598.

WANG, R., XIA, Y., GROSSER, H., WETZEL, H.-U., ZSCHAU, J., and KAUFMANN, H. (2004), The 2003 Bam (SE Iran) earthquake: Precise source parameters from satellite radar Interferometry, *Geophys. J. Int.* 159, 917-922.

YAGI, Y. (2003),
<http://iisee.kenken.go.jp/staff/Yagi/eq/Iran20031226/IRAN20031226.htm>

USGS (2003),
http://neic.usgs.gov/neis/eq_depot/2003/eq_031226/neic_cvad_q.html

